Peptide Foldamers

International Edition: DOI: 10.1002/anie.201506955
German Edition: DOI: 10.1002/ange.201506955

Turning Peptide Sequences into Ribbon Foldamers by a Straightforward Multicyclization Reaction

*Vincent Martin, Baptiste Legrand, Lubomir L. Vezenkov, Mathéo Berthet, Gilles Subra, Monique Calmès, Jean-Louis Bantignies, Jean Martinez, and Muriel Amblard**

Abstract: *The conformational control of molecular scaffolds allows the display of functional groups in defined spatial arrangement. This is of considerable interest for developing fundamental and applied systems in both the fields of biology and material sciences. Peptides afford a large diversity of functional groups, and peptide synthetic routes are very attractive and accessible. However, most short peptides do not possess well-defined secondary structures. Herein, we developed a simple strategy for converting peptide sequences into structured γ-lactam-containing oligomers while keeping the amino acids side chain diversity. We showed the propensity of these molecules to adopt ribbon-like secondary structures. The periodic distribution of the functional groups on both sides of the ribbon plane is encoded by the initial peptide sequence.*

Since the pioneering works of Gellman[1] and Seebach,[2] various foldamers have been developed based on different building blocks, which are mostly derived from natural α-amino acids, including β-, γ-, and δ-amino acid derivatives.[1,3] Peptide-like foldamers allowed the construction of numerous folded architectures, mainly determined by periodic secondary structures stabilized by intramolecular hydrogen bonds (for example, 14-, 12, 10/12-helix). The first generation of foldamers consisting of homogeneous backbones was enlarged by heterogeneous backbones containing two different types of subunits, typically a combination of α-, β-, and γ-amino acid residues.[4] β- or γ-turn motifs have also been used for generating oligomers with well-defined secondary structure orchestrated by recurrent conformationally restrained motifs.[5,6] Early works showed that sequential peptides with periodic Pro-X and X-Pro dipeptides (with X = Aib, Ala, or D-Ala residues) adopted preferentially β-bend ribbon conformations, which are considered as a subtype of 3_{10}-helix.[7] Theoretical studies using helical parameters and Ramachandran plots confirmed that successive β-turn dipeptide mimetics in proteins give rise to flat or twisted ribbon structures, depending on the type of β-turns.[8] Along with this trend, oligomers containing periodic β- or γ-turn dipeptide mimetics have been shown to retain the intrinsic conformational properties of their monomeric units within the oligomer, thus displaying regular secondary structures.[6]

Herein, we propose a strategy to generate novel folded architectures based on α-amino-γ-lactam derivatives (Agl-AA_x with AA_x = amino acid), so-called Freidinger's lactams,[9,10] widely used as type II β-turn inducers in relevant bioactive peptides.[11] This strategy has several advantages. First, only α-amino acids are used as starting material, enabling easy access to these new foldamers and the possibility of using conventional solid-phase peptide synthesis (SPPS) methods. Second, the structurally constrained blocks are generated in the course of the SPPS, avoiding the preparation of each dipeptide lactam unit prior to the construction of the oligomers. Solid-phase methods for the on-line synthesis of peptides containing a single α-amino-γ-lactam unit have been reported.[12] However, these methods required the synthesis of the lactam precursors in solution prior to their incorporation on the solid support. Therefore, we developed a method on solid support that relies on a direct conversion of target peptide sequences with alternating methionine and α-amino acid residues into a folded (Agl-AA_x)-based oligomers, via a key multicyclization step (Scheme 1). For that purpose, different oligomers alternating five-membered ring lactams (Agl) either with aromatic, basic, or the combination of aromatic/basic amino acids (AA_x), were synthesized and their ability to fold into a well-defined conformation was investigated.

Thus, a series of α-amino γ-lactam oligomers of different lengths **10a–c**, **11a–c**, and **12a–c** were generated from peptide sequences alternating methionine and phenylalanine or arginine residues (Scheme 1; see the Supporting Information for experimental procedures). All of the precursor peptide sequences were synthesized on Rink amide resin according to Fmoc/*t*Bu microwave-assisted solid-phase peptide synthesis (SPPS).[13] The free *N*-terminal amino group of the tetra, octa, and dodecapeptides H-(Met-AA_x)$_n$-NH-Rink amide were capped by 2-bromobenzyloxycarbonyl group to afford compounds **1a–c**, **2a–c**, and **3a–c**, respectively, that will subsequently undergo multi-lactamization. Prior to the solid phase synthesis of Agl-AA_x oligomers **7a–c**, **8a–c**, and **9a–c** by a multicyclization reaction, we first optimized the experimental conditions of γ-lactam ring formation[10] on solid support using the model Ac-Met-Phe-NH-Resin (Supporting Information). The conversion of the supported dipeptide unit (Ac-

[*] Dr. V. Martin,[+] Dr. B. Legrand,[+] Dr. L. L. Vezenkov, M. Berthet, Prof. G. Subra, Dr. M. Calmès, Prof. J. Martinez, Dr. M. Amblard
Institut des Biomolécules Max Mousseron (IBMM)
UMR 5247 CNRS-Université Montpellier-ENSCM,
Bâtiment E, Faculté de Pharmacie
34093 Montpellier cedex 5 (France)
E-mail: muriel.amblard@univ-montp1.fr
Homepage: http://www.ibmm.univ-montp1.fr
Prof. J.-L. Bantignies
LC2 - UMR 5221 CNRS, Université de Montpellier
Place Eugène Bataillon, 34095 Montpellier (France)
[+] These authors contributed equally to this work.

Supporting information for this article is available on the WWW under http://dx.doi.org/10.1002/anie.201506955.

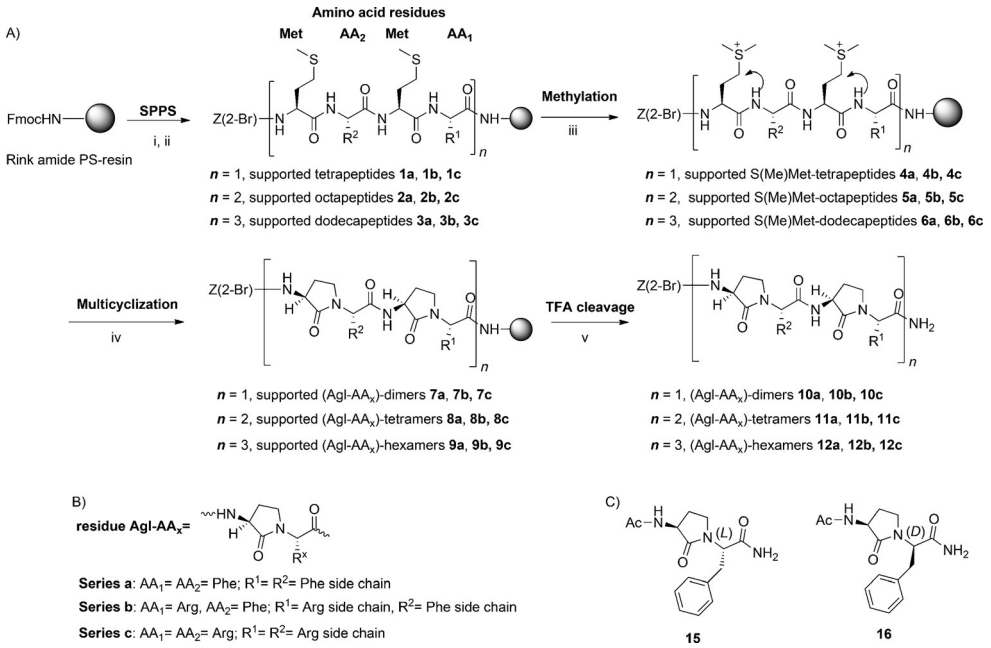

Scheme 1. A) Synthesis of Z(2-Br)-(Agl-AA$_x$)$_n$-NH$_2$ **10a–c**, **11a–c**, and **12a–c** on Rink amide-PS resin. Conditions i) SPPS: coupling: Fmoc-AA-OH (4 equiv), HBTU (4 equiv), DIEA (8 equiv), DMF; deprotection: Pip/DMF (20:80); ii) Z(2-Br)-OSu (3 equiv), NMM (3 equiv), DMF. iii) MeI (30 equiv), DMF/DCM (1:1), 24 h or 48 h. iv) 5% DBU in DMF/DCM (1:1), 48 h. v) TFA, 2 h. B) Series of (Agl-AA$_x$) oligomers and abbreviations used for α-amino-γ-lactam residue; C) Diastereoisomers **15** and **16**.

Met-Phe-NH-Resin) into its sulfonium salt by iodomethane treatment (30 equiv) in a 1:1 mixture of DCM/DMF followed by an intramolecular *N*-alkylation reaction in a solution of 5% DBU in 1:1 DCM/DMF afford, after trifluoroacetic acid (TFA) treatment, the desired Ac-Agl-Phe-NH$_2$ (compound **15**). Under these conditions, the risk of epimerization of the C-terminal phenylalanine residue was investigated. For that purpose, the diastereoisomer Ac-Met-D-Phe-NH$_2$ and its corresponding Ac-Agl-D-Phe-NH$_2$ (compound **16**) were synthesized (Supporting Information). After cleavage of the two diastereoisomers **15** and **16** from the resin by TFA treatment, comparison of the HPLC and LC/MS analyses of these compounds showed that no epimerization has occurred (Supporting Information, Scheme S1). Using the optimized conditions of methylation, **1a–c** and **2a–c** were converted into their sulfonium salt for 24 h, whereas longer peptides **3a–c** were reacted for 48 h, to afford compounds **4a–c**, **5a–c**, and **6a–c** respectively. Afterward, methionine sulfonium intermediates were subjected to multi-intramolecular *N*-alkylation reaction. The multicyclization step provided an almost total conversion of the shorter linear peptide sequences (**4a–c**, **5a–c**) into the supported cyclized sequences **7a–c**, **8a–c** within 48 h. For peptides **6a–c**, a second cycle of methylation and cyclization was necessary to reach a total conversion into compounds **9a–c**. Completion of both methylation and cyclization reactions were monitored by LC/MS analysis of the crude peptide cleaved from an aliquot of resin. Simultaneous removal of protecting groups and cleavage of the oligomers from the solid support by TFA treatment yielded crude Agl-AA$_x$ oligomers **10a–c**, **11a–c**, and **12a–c** with a purity ranging from 50% to 80%. All of the final compounds were then purified by preparative HPLC for structural studies (Supporting Information).

FT-IR, NMR, and CD spectroscopic studies were performed to characterize the conformational preference of the (Agl-AA$_x$)-based oligomers in solution.

First, extensive NMR studies of the different series of compounds dissolved in various solvents were performed. The NMR spectra of the hydrophobic oligomers **10a–12a** were recorded in [D$_5$]pyridine and CD$_3$OH while the amphipathic **10b–12b** and cationic **10c–12c** series were studied in CD$_3$OH and in aqueous media at pH 6.3 (Supporting Information, Figures S3–S8). Combination of two-dimensional homo- (COSY, TOCSY, and ROESY) and heteronuclear (^{13}C and ^{15}N-HSQC) experiments allowed us to assign the ^{1}H, ^{13}C, and ^{15}N resonances of compounds (Supporting Information, Tables S1–S9). Stereospecific assignments of the non-equivalent diastereotopic methylene groups of the lactam rings and the phenylalanine/arginine side chains where determined based on the intensities of the intra-residue NOE and the $^3J(H_\alpha,H_\beta)$ and $^3J(H_\alpha,H_{\beta'})$ coupling constants (Supporting Information, Figure S2). We detected stronger intra-residue NOE intensities between H_α and the downfield H_β, and the upfield H_γ protons of the lactam ring than between H_α and the corresponding $H_{\beta'}$ and $H_{\gamma'}$. Similarly, for the phenylalanine and arginine residue methylene groups, stronger NOE intensities were measured between H_α and the upfield H_β protons than between H_α and the upfield $H_{\beta'}$ protons, associated to small $^3J(H_\alpha,H_\beta)$ and large $^3J(H_\alpha,H_{\beta'})$ vicinal coupling constants (Supporting Information, Tables S11, S13).

The conformational preferences of the hydrophobic oligomers **10a–12a** were investigated in detail. Well-dispersed spectra for all of the compounds were obtained in [D$_5$]pyridine, despite the repetitive nature of the sequences. Obviously, we observed a lower signal dispersion in CD$_3$OH, preventing the complete resonance assignment for the longer oligomer **12a**. Furthermore, numerous $^3J(H_N,H_\alpha)$, $^3J(H_\alpha,H_\beta)$, and $^3J(H_\alpha,H_{\beta'})$ vicinal coupling constants could be accurately measured in [D$_5$]pyridine, while in CD$_3$OH, numerous signals overlapped. Nevertheless, we identified the same characteristic NOE patterns in both solvents, involving unambiguous medium- and long-range NOE correlations, weak NHi/H_β(i−2), medium NHi/H_γ(*i*−2), and weak H_αi/H_β(*i*−3), which provided evidence of conformational preferences of

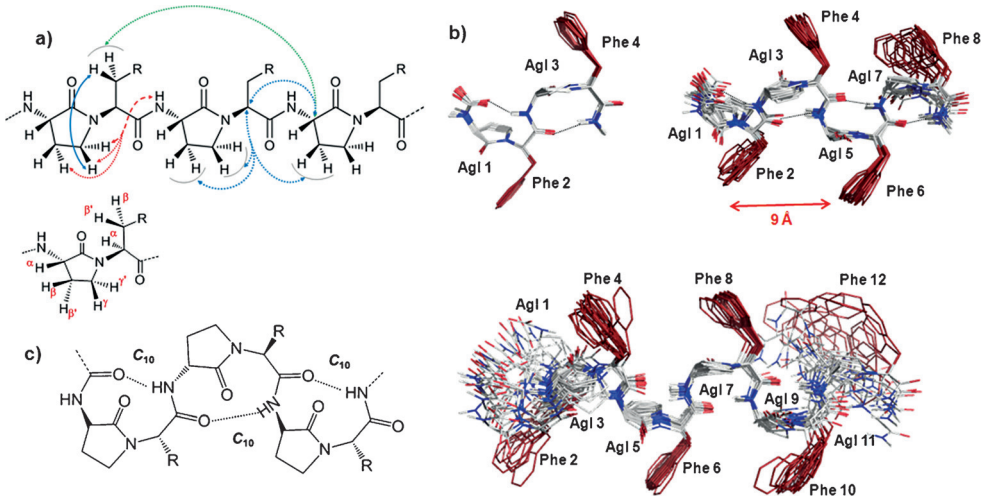

Figure 1. a) Nomenclature of the Agl-AA_x oligomers protons and characteristic NOE correlations of the $(Agl\text{-}AA_x)_n$ oligomers. "Strong", "medium", and "weak" NOEs are shown in plain, dashed, and dotted arrows, respectively. Typical sequential, medium, and long-range NOEs are in blue, red, and green, respectively. b) Superimposition of the 20 lowest-energy NMR solution structures of the Agl-Phe oligomers **10a**, **10b**, and **10c** in [D_5]pyridine. The *N*-terminal capping and hydrogen (except amide protons) have been omitted for clarity. c) Typical hydrogen-bond networks stabilizing the ribbon structures of the $(Agl\text{-}AA_x)_n$ oligomers.

the oligomers (Supporting Information, Figures S9–S10 and Tables S22–S24). Moreover, we detected stereospecific NOE connectivities between the prochiral methylene groups of the γ-lactam rings and phenylalanine side chains, which have been used to derive valuable stereospecific restraints. The calculated lowest-energy conformations of the $(Agl\text{-}Phe)_{2,4,6}$ adopted a well-defined β-ribbon structure composed of successive β-turns stabilized by C=O(i)···HN($i+3$) hydrogen bonds forming a 10-membered pseudocycle (Figure 1).

The convergence of the NMR structures was obviously lower at both extremities, in particular for the longest oligomers (Supporting Information, Table S25). The typical average backbone torsion angle ϕ and ψ values were 36° and −111° for the Agl residues, and −119° and 37° for the Phe moieties, respectively (Supporting Information, Table S26). It is noteworthy that the g^- rotamer, which is strongly preferred for the phenylalanine side chains in Agl-Phe oligomers ($\chi_1 \approx -47°$), owing to the steric clashes induced by the contiguous γ-lactams rings, is also the most populated in natural peptides (Supporting Information, Table S27). This is highlighted by strong Hα/Hβ and medium Hα/Hβ′ intra-residue correlations, stereospecific NOE connectivities with the γ-lactam cycles, as well as by the $^3J(H_\alpha, H_\beta)$ and $^3J(H_\alpha, H_{\beta'})$ values of about 5.0 and 10.8 Hz, respectively. The similar NOE pattern along the various Agl-Phe sequences in both [D_5]pyridine and CD_3OH showed that the sequence length and the nature of the solvent have little to no influence on the overall topology of the β-ribbon structure (Supporting Information, Tables S22, S23). The structures established by NMR showed that all the side chains of Agl-Phe building blocks were periodically distributed in defined spatial arrangements on both sides of the ribbon-like structure (Figure 1). Side chains belonging to [Agl-Phe] and $[Agl\text{-}Phe]_{n+2}$ are aligned and separated by a distance of approximately 9 Å. A similar arrangement was found in azidoproline-containing oligoproline systems that were post-functionalized for biological or material applications.[14] In the case of Agl-AA_x oligomers, a large diversity of functional groups could be easily introduced thanks to the initial Met/AA_x peptide sequence, thus providing a large variety of structured oligomers without further post-functionalization.

The mid infrared (MIR) absorption spectra (4000–400 cm^{-1}) were then recorded in $CHCl_3$ solution to sustain the presence of intramolecular hydrogen bonds that stabilize the repeating β-turn conformation in Agl-Phe oligomers. The frequencies of both the amide A ν(NH) and amide I vibrations ν(CO) are classically downshifted when the hydrogen bonds are strengthened.[15] In the ν(NH) region (3600–3100 cm^{-1}), oligomers **10a**–**12a** exhibited two main amide contributions, one above 3450 cm^{-1} and one below 3350 cm^{-1}, corresponding to non-hydrogen bonded and hydrogen bonded NH, respectively (Figure 2). According to the NMR structures, the intensity of the H-bonded amide band (ν_{HB}(NH)) increased with the oligomer length, owing to an increase in the intramolecular H-bonding rate. The downshift of the ν_{HB}(NH) band position to lower frequencies, along with the increase of the oligomer size (from 3340 to 3306 cm^{-1}), suggests a cooperative effect with stronger hydrogen bonds. In the free amide range (above 3400 cm^{-1}), the complex band with two maxima at 3474 and 3461 cm^{-1} is consistent with the presence of free N-H of the C-terminal amide and free NH-terminal urethane. In the amide I region (1800–1600 cm^{-1}), while the high frequency band around 1697 cm^{-1} was assigned to intra-cyclic C=O group (ν_{cyc}(CO)), not engaged in H-bond, the band near 1660 cm^{-1} corresponded to the amide C=O group engaged in H-bond (ν_{HB}(CO)). As expected, we observed a concomitant increase of the intensity bands of both ν_{HB}(CO) and ν_{cyc}(CO)

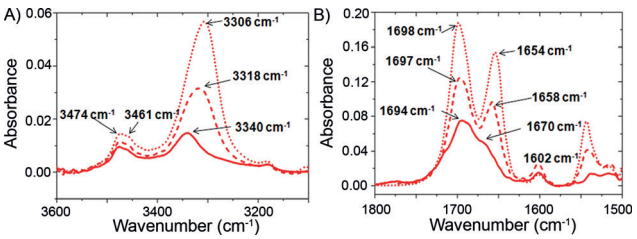

Figure 2. FTIR spectra of compounds **10a**–**12a** at 1 mM in $CHCl_3$. Compound **10a** is indicated by a plain line, **11a** by a dashed line, and **12a** by a dotted line. A) Amide A and B) amide I region

with the oligomer length. In agreement with the ν_{HB}(NH) behavior, the ν_{HB}(CO) band position was downshifted when the oligomer lengths increased, while the position of ν_{cyc}(CO) band position remained almost unchanged. The ν_{HB}(CO) and ν_{HB}(NH) behaviors appeared deeply correlated, supporting the progressive establishment of an intramolecular hydrogen bonding network when the size of the oligomer increased.

The deconvolution ν(CO) and ν(NH) bands of the oligomers (Supporting Information, Figure S11) allowed us to quantify the ratios between the free and H-bonded amide species (Supporting Information, Tables S30–S32). It is noteworthy that the ratios obtained from IR data were similar with those expected for oligomers adopting a β-ribbon structure. For example, in $(Agl\text{-}Phe)_n$ (compounds **10a**–**12a**), the percentages of bound NH determined from IR experimental analysis increased with the oligomer length from 50% ($n=2$) to 75% ($n=6$), as expected from the NMR data. We globally found a good correlation between the ratio of free and H-bonded NH and C=O in the structures calculated under NMR restraints and estimated from IR analysis.

In the next step, we addressed whether the amphipathic $(Agl\text{-}Phe/Arg)_n$ **10b**–**12b** and cationic $(Agl\text{-}Arg)_n$ **10c**–**12c** oligomers also adopted a ribbon structure in methanol and in water. First, an IR absorption study of compounds **11b** and **11c**, as amphipatic and cationic model oligomers in D_2O was carried out. While strong absorption bands of the solvent prevented the interpretation of the amide A region; we observed for both compounds a complex band with three main components in the amide I region (Supporting Information, Figure S12). The low and high frequency shoulders at 1690 and 1653 cm^{-1} corresponded respectively to ν_{cyc}(CO) and ν_{HB}(CO), and the main contribution at 1673 cm^{-1} was assigned to guanidinium vibration.[16] The band deconvolution indicated the presence of similar proportions of the free NH amides and H-bonded NH amides in D_2O compared to Agl-Phe tetramers in $CHCl_3$ (Supporting Information, Figure S13), suggesting that the Agl-AA_x amphipathic and cationic tetramers still adopted a folded structure involving hydrogen bonds in D_2O.

Afterwards, we carefully searched for the characteristic NOE pattern detected for the **10a**–**12a** $(Agl\text{-}Phe)_n$ oligomers in [D_5]pyridine and CD_3OH, in the ROESY spectra of the amphibatic $(Agl\text{-}Phe/Arg)_n$ **10b**–**12b** and cationic $(Agl\text{-}Arg)_n$ **10c**–**12c** oligomers in both CD_3OH and water (pH 6.3). All of the ^1H, ^{13}C, and ^{15}N resonances of the two series of oligomers were assigned in CD_3OH, while significant signal overlaps in H_2O/D_2O prevented the complete assignment of resonances of the $(Agl\text{-}Phe/Arg)_{12}$ and of the repetitive $(Agl\text{-}Arg)_{8,12}$ oligomers. Despite the low quality of these spectra, a notable amount of typical NOEs were also found in CD_3OH and in water (Supporting Information, Tables S28, S29).

Furthermore, we performed a circular dichroism (CD)study on aliphatic oligomers **10a**–**12a** in CH_3OH, and in both CH_3OH and water for amphipatic **10b**–**12b** and cationic oligomers, **10c**–**12c** (Figure 3; Supporting Information, Figures S36, S37). We observed similar signatures regardless of the nature of the oligomers (hydrophobic, amphipathic, or polycationic), with a large negative band at about 224 nm and a slight shoulder around 208 nm in CH_3OH (Figure 3B). In water, amphipatic and cationic compounds displayed similar CD signatures with a slightly shifted minimum near 222 nm. There was also a maximum at about 193 nm that was not observed in CH_3OH, owing to the strong absorption of the solvent at this wavelength. These data indicate that (Agl-AA_x)-based oligomers share a similar conformation in CH_3OH and in water, and importantly, point out the stability of amphipatic and cationic oligomer structures in aqueous media. Interestingly, the per-unit molar ellipticity value of the minimum did not increase markedly with the number of monomers, supporting the idea that the ribbon structure was governed by each pre-organized Agl-AA_x β-turn unit which was retained within the oligomers (Figure 3A). Considering the Agl-Phe series, we only noticed a slight increase of the Cotton effect at 224 nm between the dimer **10a** and the tetramer **11a**, with no significant difference between **11a** and the hexamer **12a**. These results are consistent with the FTIR data (Figure 2). Indeed, whereas amide I band of tetramer **11a** and hexamer **12a** presented similar band shapes, the dimer **10a** band exhibited a high frequency shoulder, suggesting an enhanced dispersion of hydrogen bond strengths. Furthermore, both ν_{HB}(CO) and ν_{HB}(NH) band positions of the dimer are upshifted compared to others oligomers, also supporting weaker intramolecular H-bonds in this case. In this context, although the dimer presents more heterogeneous H-bonding strengths than the longer oligomers, no strong cooperative effect with the oligomer size occurred for the Agl-AA_x ribbon.

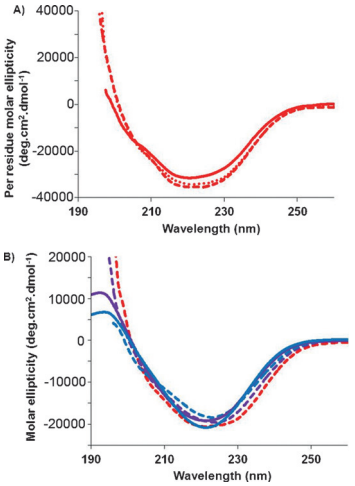

Figure 3. A) CD spectra of (Agl-Phe) dimer (plain line), tetramer (dashed), and hexamer (dotted) in methanol at 20°C. B) CD spectra of $(Agl\text{-}Phe)_6$ in red, $(Agl\text{-}Phe/Arg)_6$ in purple, and $(Agl\text{-}Arg)_6$ in blue. Spectra were recorded in methanol (dashed) and in water, pH 6.3 (plain lines).

Finally, considering the FTIR, CD, and NMR data in water together, we could conclude that the Agl-AA_x amphipatic and cationic series retained the β-ribbon structure in aqueous media.

In conclusion, we have developed a straightforward and unprecedented way to obtain α-amino-γ-lactam-based foldamers from simple peptide sequences by alternating methionine and α-amino acid residues in a 1:1 pattern. Interestingly,

the key step of multicyclization of the peptide sequence proceeds on solid support with a complete conversion into the α-amino-γ-lactam oligomer. Conformational investigations by NMR, FTIR, and CD showed the ability of these oligomers to fold into a well-defined repeating-turn secondary structure stabilized by $(i, i+3)$ inter-residue hydrogen bonds in solution. The periodic distribution of side chains on both sides of the plane of the ribbon was controlled by the initial peptide sequence. Such compounds allow the display of functional groups in defined spatial arrangement. The strategy could be considered for converting a whole target peptide sequence, or only a desired part of a peptide sequence, into structured peptide scaffolds for specific applications including antimicrobial or cell-membrane permeable compounds. Agl-AA_x oligomers could be also used as scaffolds for multivalent biological targeting.

Acknowledgements

The authors thank the Fondation pour la Recherche Médicale (FRM DCM20121225739) for financial support. SynBio3 IBISA and SIMS platforms; and LMP (Laboratoire de Mesures Physiques) are also thanked for providing access to peptide synthesis, IR, NMR and CD facilities.

Keywords: α-amino-γ-lactams · foldamers · multicyclization · ribbon-like structure · solid supported synthesis

How to cite: *Angew. Chem. Int. Ed.* **2015**, *54*, 13966–13970
Angew. Chem. **2015**, *127*, 14172–14176

[1] S. H. Gellman, *Acc. Chem. Res.* **1998**, *31*, 173–180.
[2] D. Seebach, A. K. Beck, D. J. Bierbaum, *Chem. Biodiversity* **2004**, *1*, 1111–1239.
[3] a) D. J. Hill, M. J. Mio, R. B. Prince, T. S. Hughes, J. S. Moore, *Chem. Rev.* **2001**, *101*, 3893–4011; b) C. M. Goodman, S. Choi, S. Shandler, W. F. DeGrado, *Nat. Chem. Biol.* **2007**, *3*, 252–262; c) A. D. Bautista, C. J. Craig, E. A. Harker, A. Schepartz, *Curr. Opin. Chem. Biol.* **2007**, *11*, 685–692; d) Foldamers: Structure, Properties, and Applications. (Eds.: S. Hecht, I. Huc), Wiley-VCH, Weinheim, **2007**; e) R. P. Cheng, S. H. Gellman, W. F. DeGrado, *Chem. Rev.* **2001**, *101*, 3219–3232.
[4] a) S. De Pol, C. Zorn, C. D. Klein, O. Zerbe, O. Reiser, *Angew. Chem. Int. Ed.* **2004**, *43*, 511–514; *Angew. Chem.* **2004**, *116*, 517–520; b) A. Hayen, M. A. Schmitt, F. N. Ngassa, K. A. Thomasson, S. H. Gellman, *Angew. Chem. Int. Ed.* **2004**, *43*, 505–510; *Angew. Chem.* **2004**, *116*, 511–516; c) G. V. M. Sharma, P. Nagendar, P. Jayaprakash, P. R. Krishna, K. V. S. Ramakrishna, A. C. Kunwar, *Angew. Chem. Int. Ed.* **2005**, *44*, 5878–5882; *Angew. Chem.* **2005**, *117*, 6028–6032; d) G. Srinivasulu, S. K. Kumar, G. V. M. Sharma, A. C. Kunwar, *J. Org. Chem.* **2006**, *71*, 8395–8400; e) D. Seebach, B. Jaun, R. Sebesta, R. I. Mathad, O. Flogel, M. Limbach, H. Sellner, S. Cottens, *Helv. Chim. Acta* **2006**, *89*, 1801–1825; f) W. S. Horne, S. H. Gellman, *Acc. Chem. Res.* **2008**, *41*, 1399–1408; g) P. G. Vasudev, S. Chatterjee, N. Shamala, P. Balaram, *Chem. Rev.* **2011**, *111*, 657–687; h) L. K. A. Pilsl, O. Reiser, *Amino Acids* **2011**, *41*, 709–718; i) B. Legrand, C. Andre, L. Moulat, E. Wenger, C. Didierjean, E. Aubert, M. C. Averlant-Petit, J. Martinez, M. Calmes, M. Amblard, *Angew. Chem. Int. Ed.* **2014**, *53*, 13131–13135; *Angew. Chem.* **2014**, *126*, 13347–13351.
[5] a) J. S. Madalengoitia, *J. Am. Chem. Soc.* **2000**, *122*, 4986–4987; b) N. Castellucci, C. Tomasini, *Eur. J. Org. Chem.* **2013**, 3567–3573.
[6] a) C. Tomasini, G. Luppi, M. Monari, *J. Am. Chem. Soc.* **2006**, *128*, 2410–2420; b) D. Srinivas, R. Gonnade, S. Ravindranathan, G. J. Sanjayan, *J. Org. Chem.* **2007**, *72*, 7022–7025; c) P. K. Baruah, N. K. Sreedevi, R. Gonnade, S. Ravindranathan, K. Damodaran, H. J. Hofmann, G. J. Sanjayan, *J. Org. Chem.* **2007**, *72*, 636–639; d) C. Tomasini, G. Angelici, N. Castellucci, *Eur. J. Org. Chem.* **2011**, 3648–3669; e) M. D. Smith, T. D. W. Claridge, M. S. P. Sansom, G. W. J. Fleet, *Org. Biomol. Chem.* **2003**, *1*, 3647–3655.
[7] a) Y. V. Venkatachalapathi, P. Balaram, *Biopolymers* **1981**, *20*, 1137–1145; b) B. V. Venkataram Prasad, P. Balaram, *Int. J. Biol. Macromol.* **1982**, *4*, 99–102; c) I. L. Karle, J. Flippenanderson, M. Sukumar, P. Balaram, *Proc. Natl. Acad. Sci. USA* **1987**, *84*, 5087–5091; d) B. Di Blasio, V. Pavone, M. Saviano, A. Lombardi, F. Nastri, C. Pedone, E. Benedetti, M. Crisma, M. Anzolin, C. Toniolo, *J. Am. Chem. Soc.* **1992**, *114*, 6273–6278.
[8] S. Hayward, D. P. Leader, F. Al-Shubailly, E. J. Milner-White, *Proteins Struct. Funct. Bioinf.* **2014**, *82*, 230–239.
[9] R. M. Freidinger, D. F. Veber, D. S. Perlow, J. R. Brooks, R. Saperstein, *Science* **1980**, *210*, 656–658.
[10] R. M. Freidinger, D. S. Perlow, D. F. Veber, *J. Org. Chem.* **1982**, *47*, 104–109.
[11] a) A. Perdih, D. Kikelj, *Curr. Med. Chem.* **2006**, *13*, 1525–1556; b) R. M. J. Liskamp, D. T. S. Rijkers, J. A. W. Kruijtzer, J. Kemmink, *ChemBioChem* **2011**, *12*, 1626–1653.
[12] a) W. L. Scott, J. Alsina, J. H. Kennedy, M. J. O'Donnell, *Org. Lett.* **2004**, *6*, 1629–1632; b) T. Lama, P. Campiglia, A. Carotenuto, L. Auriemma, I. Gomez-Monterrey, E. Novellino, P. Grieco, *J. Pept. Res.* **2005**, *66*, 231–235; c) A. G. Jamieson, N. Boutard, K. Beauregard, M. S. Bodas, H. Ong, C. Quiniou, S. Chemtob, W. D. Lubell, *J. Am. Chem. Soc.* **2009**, *131*, 7917–7927.
[13] M. Amblard, J. A. Fehrentz, J. Martinez, G. Subra, *Mol. Biotechnol.* **2006**, *33*, 239–254.
[14] a) M. Kümin, L. S. Sonntag, H. Wennemers, *J. Am. Chem. Soc.* **2007**, *129*, 466–467; b) G. Upert, F. Bouillere, H. Wennemers, *Angew. Chem. Int. Ed.* **2012**, *51*, 4231–4234; *Angew. Chem.* **2012**, *124*, 4307–4310; c) Y. A. Nagel, M. Kuemin, H. Wennemers, *Chimia* **2011**, *65*, 264–267; d) C. Kroll, R. Mansi, F. Braun, S. Dobitz, H. R. Maecke, H. Wennemers, *J. Am. Chem. Soc.* **2013**, *135*, 16793–16796; e) U. Lewandowska, W. Zajaczkowski, L. Chen, F. Bouillière, D. P. Wang, K. Koynov, W. Pisula, K. Mullen, H. Wennemers, *Angew. Chem. Int. Ed.* **2014**, *53*, 12537–12541; *Angew. Chem.* **2014**, *126*, 12745–12749.
[15] a) J. L. Bantignies, L. Vellutini, J. L. Sauvajol, D. Maurin, M. W. C. Man, P. Dieudonne, J. J. E. Moreau, *J. Non-Cryst. Solids* **2004**, *345*, 605–609; b) G. Creff, B. P. Pichon, C. Blanc, D. Maurin, J. L. Sauvajol, C. Carcel, J. J. E. Moreau, P. Roy, J. R. Bartlett, M. W. C. Man, J. L. Bantignies, *Langmuir* **2013**, *29*, 5581–5588.
[16] a) Y. N. Chirgadze, O. V. Fedorov, N. P. Trushina, *Biopolymers* **1975**, *14*, 679–694; b) S. Y. Venyaminov, N. N. Kalnin, *Biopolymers* **1990**, *30*, 1243–1257.

Received: July 27, 2015
Revised: August 26, 2015
Published online: September 23, 2015

